RAPID COMMUNICATIONS

PHYSICAL REVIEW B VOLUME 51, NUMBER 1 1 JANUARY 1995-I

Neutron-diffraction study of antiferromagnetic order in the magnetic superconductor $ErNi_2B_2C$

S. K. Sinha
Corporate Research, Exxon Research & Engineering Company, Annandale, New Jersey 08801

J. W. Lynn and T. E. Grigereit
Reactor Radiation Division, National Institute of Standards & Technology, Gaithersburg, Maryland 20899
and Department of Physics, University of Maryland, College Park, Maryland 20742

Z. Hossain, L. C. Gupta, and R. Nagarajan
Tata Institute of Fundamental Research, Bombay 400 005, India

C. Godart
CNRS, UPR-209, 92195 Meudon, Cedex, France
(Received 19 September 1994)

We have carried out powder-neutron-diffraction studies of the antiferromagnetic order that develops below $T_N = 6.8$ K in the magnetic superconductor ($T_c = 11$ K) $ErNi_2B_2C$. The antiferromagnetic structure is associated with spins on the Er atoms, which order in a transversely polarized planar sinusoidal structure propagating along the a or b axis in equal domains, with the Er moments parallel to the b or a axis, respectively. Third and fifth harmonics of the sine wave are observed at low temperatures, indicating a squared-up sine wave, with a low-temperature amplitude of $7.8\mu_B$/Er atom. There is also evidence of an induced moment of $-0.35\mu_B$ on the Ni ions. A similar study of the isostructural compound YNi_2B_2C revealed no magnetic peaks ($\mu < 0.13\mu_B$) developing down to 0.3 K for Q values less than 1.6 $Å^{-1}$.

Several recent studies have been reported on superconductivity in the family of quaternary intermetallic compounds with the formula RNi_2B_2C (R=Y, or a lanthanide atom),[1–5] with T_c as high as 16.6 K for $LuNi_2B_2C$ and 15.6 K for YNi_2B_2C and lower values for the compounds containing magnetic lanthanide atoms. The crystal structure for these compounds is a body-centered tetragonal (bct) structure similar to the $ThCr_2Si_2$-type system with an additional carbon atom in each lanthanide layer.[4,6] Electronic band-structure calculations for these materials show[7–9] them to have Fermi levels slightly above a cluster of peaks in the electronic density of states associated predominantly with the Ni 3d bands, with a relatively high density of states at E_F, and it has been suggested that these are conventional superconductors with relatively strong electron-phonon coupling; at least some of these features are born out by experiment.[10,11] For the compounds containing magnetic lanthanide atoms, these systems afford the possibility of studying the interplay of magnetism and superconductivity previously studied in the Chevrel-phase compounds,[12,13] in $ErRh_4B_4$,[14,15] and to a lesser extent, in the magnetic lanthanide-containing high-T_c cuprate superconductors.[16] In the case of $HoNi_2B_2C$, interesting effects have been observed below T_c associated with the development of magnetic order. Initially a long-wavelength spiral magnetic structure develops, which drives the system normal as the ordered moment increases. Then a lock-in transition to a commensurate antiferromagnetic structure of alternating ferromagnetic sheets of Ho atoms occurs, that permits the return of superconductivity and coexistence with the antiferromagnetic order down to the lowest temperatures.[17,18] For $ErNi_2B_2C$, no such reentrant normal phase appears below the superconducting transition of $T_c \sim 11$ K. The antiferromagnetic structure which develops at $T_N = 6.8$ K is, however, always incommensurate and does not display ferromagnetic basal-plane sheets of Er atoms. The staggered magnetization increases smoothly as the temperature is decreased below T_N and is nonhysteretic.

The sample was prepared by melting the elements Y or Er (purity 99.9%), Ni (99.9%), B (99.8%), and C (99.7%) in an arc-furnace under a protective atmosphere of flowing argon. First, Er (or Y), Ni, and B were melted together, and then carbon was added and the alloy was melted four times. The overall loss in weight of the sample was less than 1%. The sample was characterized by x-ray diffraction and was found to be predominantly single phase, with a few weak impurity phase peaks with intensities less than a few percent of the strong $ErNi_2B_2C$ peaks. Superconductivity was checked by ac susceptibility, and the diamagnetic response compared very favorably with that of a piece of lead of comparable size. The pellets of $ErNi_2B_2C$ and YNi_2B_2C were crushed into powders and placed in thin rectangular sample containers of dimension $49 \times 29 \times 1$ mm^3 in order to reduce the effects of absorption. Each container was then mounted in a pumped ^{4}He cryostat for the neutron-diffraction experiments. The measurements were carried out at the Research Reactor of the National Institute of Standards and Technology on the BT-9 spectrometer, using the standard configuration of a graphite monochromator and an incident wavelength of 2.376 Å, with 48′ collimation before and after the sample. A pyrolytic graphite filter was used to remove higher-order contamination of the incident beam.

Figure 1(a) shows the powder diffraction pattern obtained at 10 K, above the magnetic ordering temperature. The

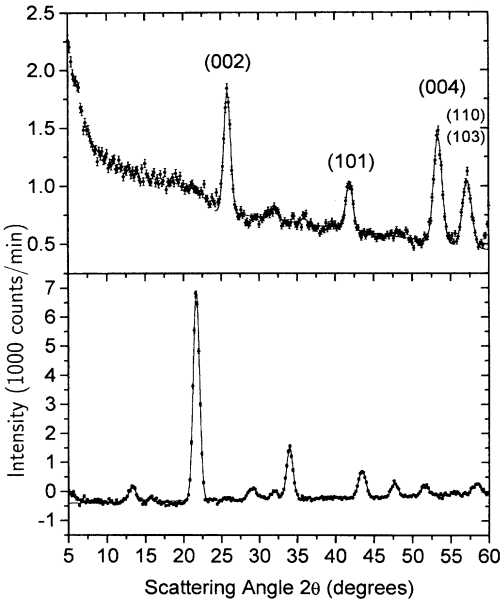

FIG. 1. The powder-diffraction pattern for $ErNi_2B_2C$ at 10 K (top), showing the nuclear diffraction peaks. The bottom part of the figure is a subtraction of the 10 K data from the data at 2 K, and reveals the magnetic diffraction pattern as indexed in Table I.

nuclear Bragg peaks from the known RNi_2B_2C structure are indicated in the Fig. 1, and we can also see some weak additional scattering arising from impurities. The integrated intensities of the higher-order peaks appear to be suppressed considerably below the values calculated from the nuclear structure factors, assuming an identical crystal structure to $HoNi_2B_2C$.[6] Accordingly, an empirical angle-dependent absorption correction factor (to allow for the considerable absorption due to the natural boron in the sample) was estimated from a comparison of the observed and calculated integrated intensities. As the temperature was lowered, extra broad peaks corresponding to magnetic short-range order or critical scattering appeared, and below 6.8 K developed into sharp resolution-limited diffraction peaks. Figure 1(b) shows the difference pattern between the diffraction pattern at 2 K and that at 10 K, which reveals the additional peaks due to the antiferromagnetic ordering of the Er ions. As a consistency check we note that the nuclear Bragg peaks (as well as the impurity peaks) cancel from such a subtraction, as they should if there is no observable *ferromagnetic* component to the magnetic ordering. From the widths of the peaks, which are the same as those of the nuclear peaks, we conclude that long-range antiferromagnetic order has been established.

Figure 2 shows the intensity of the most intense magnetic diffraction peak at $2\theta=21.67°$ as a function of temperature. A baseline background has been subtracted. We note that there is no significant hysteresis observable, in contrast to the case of the reentrant $HoNi_2B_2C$.[17] We have fit a mean-field theory to the data, restricting the fitted data to temperatures ≤ 5.5 K to avoid contributions from critical scattering. A Brillouin function for $J=\frac{15}{2}$ gave a poor fit to the data, which decrease much more rapidly near T_N. However, crystal-field effects are very likely important, and the magnetic ground state is most probably a doublet ($J=\frac{1}{2}$). Using mean-field

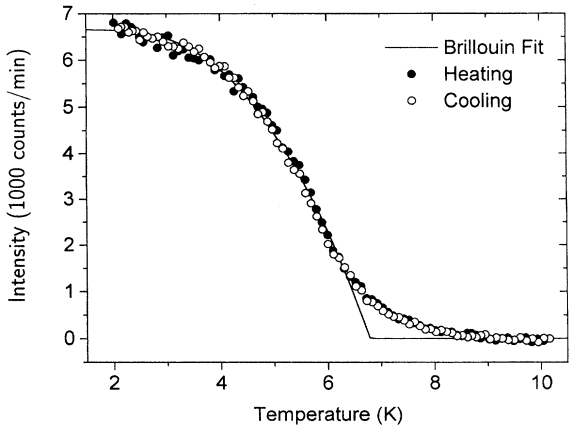

FIG. 2. The intensity of the magnetic reflection at $2\theta=21.67°$ as a function of temperature, and an empirical Brillouin function curve ($J\cong 0$) used as an interpolation formula to estimate $T_N=6.8$ K. A constant background level well above T_N has been subtracted.

theory with $J=\frac{1}{2}$ gave a reasonable fit to the data, while allowing both J and T_N to vary gave a somewhat better fit (solid curve shown) with $J\sim 10^{-3}$ and a $T_N=6.8$ K. Additional intensity due to critical scattering is seen in the vicinity of T_N. The magnetic intensity vs temperature shows no hysteresis effects on warming or cooling.

The peaks of the difference pattern can be indexed as $(h+nq_0,k,l)$ or $(h,k+nq_0,l)$ where $q_0=0.5526$, $n=\pm 1$, ± 3, or ± 5, and $(h+k+l)$ is even, i.e., a spin structure modulated along the a or b axis with a wave vector of magnitude $0.5526(2\pi/a)$, together with higher harmonics of the structure. In order to fit the integrated intensities of the magnetic powder peaks, three models were tested, initially assuming magnetic moments on the Er ions only. These were (1) a uniform spiral with the moments in the basal plane, and with spiral wave vectors along a and b axes in equal domains, with the third and fifth harmonics corresponding to "bunching" of the spiral about the fourfold axes in the basal plane; (2) a plane-wave sinusoidal structure with the moments in the basal plane and transverse to the propagation direction of the sine wave (again, along a and b axes in equal domains); and (3) model 2, but with the moments parallel to the c axis. In models (2) and (3), the higher harmonics would correspond to a "squaring up" of the sine-wave structure.

Only model (2) provided reasonable agreement with the observed intensities. In addition, the agreement was somewhat improved by including a small moment on the Ni sites as well; higher harmonics of the Ni moments were neglected. The moment on an atom at position $\boldsymbol{\kappa}$ in the unit cell $\boldsymbol{\lambda}$ for a particular domain is given by

$$\boldsymbol{\mu}(\boldsymbol{\lambda},\boldsymbol{\kappa})=\sum_n \boldsymbol{\mu}_n(\boldsymbol{\kappa})e^{in\mathbf{q}_0\cdot(\boldsymbol{\lambda}+\boldsymbol{\kappa})}+\text{c.c.} \qquad (1)$$

where $\mathbf{q}_0=(q_0,0,0)$ is the modulation vector of the antiferromagnetic structure and n represents the order of the harmonic with amplitude μ_n for the κth atom in the cell. For the three models we have

$$\text{model (1)}, \quad \boldsymbol{\mu}_n(\boldsymbol{\kappa}) = \frac{\mu_n(\boldsymbol{\kappa})}{2}(\hat{\mathbf{x}} + i\hat{\mathbf{y}})$$

$$\text{model (2)}, \quad \boldsymbol{\mu}_n(\boldsymbol{\kappa}) = \frac{\mu_n(\boldsymbol{\kappa})}{2}\hat{\mathbf{y}} \tag{2}$$

$$\text{model (3)}, \quad \boldsymbol{\mu}_n(\boldsymbol{\kappa}) = \frac{\mu_n(\boldsymbol{\kappa})}{2}\hat{\mathbf{z}}$$

and $\hat{\mathbf{x}}$, $\hat{\mathbf{y}}$, and $\hat{\mathbf{z}}$ are unit vectors along the **a**, **b**, and **c** axes, respectively. By the usual theory of magnetic diffraction,[19] the square of the magnetic structure factor for the nth harmonic is

$$|F_{\text{mag}}|_n^2 = \left(\frac{e^2\gamma}{2mc^2}\right)^2 \left| \sum_{\kappa} \{\boldsymbol{\mu}_n(\boldsymbol{\kappa}) - \hat{\mathbf{Q}}[\hat{\mathbf{Q}}\cdot\boldsymbol{\mu}_n(\hat{\boldsymbol{\kappa}})]\} \times e^{i\mathbf{G}\cdot\boldsymbol{\kappa}} f_\kappa e^{-W_\kappa} \right|^2 \tag{3}$$

where $\mathbf{G}$ is the reciprocal lattice vector (h,k,l), $\hat{\mathbf{Q}}$ is a unit vector along the wave-vector transfer $\mathbf{Q}$, f_κ the corresponding magnetic form factor for the magnetic atom κ, and e^{-W_κ} the corresponding Debye-Waller factor [obtained from a structural analysis of $HoNi_2B_2C$ (Ref. 6) and assuming that the thermal factors for Ho and Er are the same]. For model (2) Eq. (3) reduces to

$$|F_{\text{mag}}|^2 = \left(\frac{e^2\gamma}{2mc^2}\right)^2 [1-\hat{Q}_y^2] \left| \sum_{\kappa} e^{i\mathbf{G}\cdot\boldsymbol{\kappa}} \frac{\mu_n(\kappa)}{2} f_\kappa e^{-W_\kappa} \right|^2 . \tag{4}$$

For model (1) the factor $[1-\hat{Q}_y^2]$ in Eq. (4) is replaced by $[1+\hat{Q}_z^4]$, while for model (3) it is replaced by $[1-\hat{Q}_z^2]$. The integrated intensity for a peak indexed as $(h+nq_0,k,l)$ in the case of a flat sample completely bathed in radiation is then

$$I = C\,\frac{1}{2}\,\frac{|F_{\text{mag}}|^2}{\sin(\theta_B)\sin(2\theta_B)}\,jT_{\text{abs}} \tag{5}$$

where C is a constant for all the peaks, j is the multiplicity factor for the reflection, and T_{abs} is the absorption correction factor as obtained empirically from the nuclear diffraction peaks. The factor of $\frac{1}{2}$ in Eq. (2) comes from the domains. Models (1) and (3) showed deviations of factors up to 3 for some of the peaks, and were rejected. Table I lists the calculated and observed integrated intensities (the latter corrected empirically for absorption using the nuclear peak intensities, as discussed above) using model (2).

Comparing the intensities of the magnetic peaks with the nuclear Bragg peaks, we obtain values for the amplitudes of the sinusoidal moments at 2 K: $\mu_1 = 7.8\mu_B$, $\mu_3 = 0.30\mu_B$, $\mu_5 = 0.16\mu_B$, for the Er moments, and $\mu_1 = -0.35\mu_B$ for the Ni moments. Thus, the sinusoidal structure is by no means completely squared up. A schematic of the spin structure is shown in Fig. 3 for one of the domains. The unit cell is almost doubled along the a axis, but the structure is not quite commensurate.

Incommensurate spin structures have previously been observed in $ErRh_4B_4$ (Ref. 15) and $HoMo_6(S,Se)_8$,[20] but these

TABLE I. Comparison of calculated and observed magnetic Bragg peak intensities.

Peak position (2θ) (deg)	Indexing	Corrected integrated intensity	Calculated intensity
13.25	$\bar{2}00+3\mathbf{q}$	633.59	788.72
15.83	$\bar{3}01+5\mathbf{q}$	244.37	244.37
21.67	$\mathbf{q}$	7649.97	7905.30
	$\bar{1}01+\mathbf{q}$		
29.07	$\bar{2}02+3\mathbf{q}$	629.33	623.98
	$\bar{1}01+3\mathbf{q}$		
33.96	$002+\mathbf{q}$	2592.35	2545.43
43.43	$\bar{1}10+\mathbf{q}$	2142.10	1486.93
	$\bar{1}03+\mathbf{q}$		
	$\bar{2}11+3\mathbf{q}$		
47.67	$011+\mathbf{q}$	1068.76	701.97
	$\bar{1}10+3\mathbf{q}$		
	$\bar{1}03+3\mathbf{q}$		
51.59	$\bar{1}12+\mathbf{q}$	980.57	526.15
58.36	$\bar{2}00+\mathbf{q}$	1495.18	855.20
	$004+\mathbf{q}$		

are long-wavelength modulations of a ferromagnetic structure driven by the requirements of maintaining bulk superconductivity,[21,22] and the magnetic intensity showed hysteretic behavior. In $HoNi_2B_2C$, a similar long-wavelength spiral is observed,[17,18] associated with the interplay between the magnetism and the superconductivity, although for reasons that are not entirely clear at present. In a single-crystal experiment on $HoNi_2B_2C$ an additional incommensurate modulation almost doubling the unit cell along the a axis was observed,[18] as found in the present material, but was not

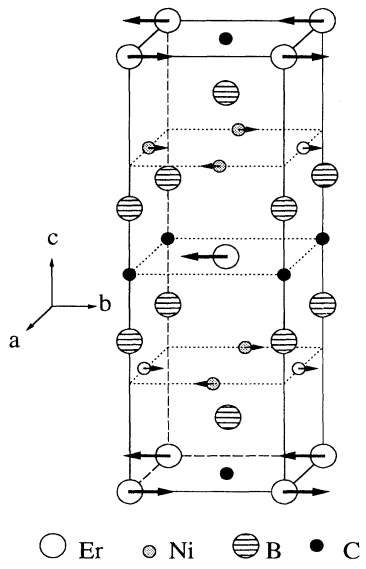

FIG. 3. Schematic of the antiferromagnetic structure of $ErNi_2B_2C$, shown for a domain with the incommensurate **q** vector along the **a** axis. Note that since the Er moment is ~22 times larger than the Ni moment they have not been drawn to scale.

found in a powder sample.[17] It is likely that in these compounds there are Fermi-surface nesting features along the a (and b) axes, which lead to the rare-earth ions ordering in a sinusoidal structure via the usual Ruderman-Kittel-Kasuya-Yosida mechanism.[9] The fact that the superconducting transition temperatures of the compounds containing magnetic rare-earth ions are lower than those of $LuNi_2B_2C$ and YNi_2B_2C indicates that there is significant exchange coupling between the magnetic f electrons and the conduction electrons. Thus, the material presumably develops both superconducting and antiferromagnetic gaps at the Fermi level, with the magnetic wave vector being determined self-consistently by the net conduction electron bands. In our analysis, a small moment on the Ni atoms, oppositely directed to the Er moments, is found to marginally improve the agreement with the experimentally observed intensities, although the existence of such a moment should be regarded as tentative until more accurate work is done using polarized neutrons or single crystals.

Powder-diffraction scans were also carried out on the analogous compound YNi_2B_2C to search for possible magnetic ordering of the Ni. Data were collected for $Q \leq 1.6$ $Å^{-1}$, and showed no magnetic diffraction peaks down to 0.3 K. The data place an upper limit of $0.13\mu_B$ for the possible Ni magnetic moment associated with any antiferromagnetic ordering. Thus, it appears that the Ni moment in the superconducting compound $ErNi_2B_2C$ is driven by the ordering of the Er moments (which presumably produce antiferromagnetic gaps at the Fermi level in the ordered state).

Magnetic diffraction studies of an $ErNi_2B_2C$ single crystal were simultaneously carried out by the Ames Laboratory group, with very similar results to ours. We are grateful to C. Stassis, A. Goldman, and P. C. Canfield for discussing their single-crystal results with us prior to publication. We would also like to thank C. M. Varma for helpful conversations. Research at Maryland was supported by the NSF, Grant No. DMR 93-02380.

[1] R. Nagarajan *et al.*, Phys. Rev. Lett. **72**, 274 (1994).
[2] R. J. Cava *et al.*, Nature (London) **367**, 146 (1994).
[3] R. J. Cava *et al.*, Nature (London) **367**, 252 (1994).
[4] T. Siegrist *et al.*, Nature (London) **367**, 254 (1994).
[5] P. C. Canfield *et al.* (unpublished).
[6] Q. Huang *et al.*, Phys. Rev. B (to be published).
[7] W. E. Pickett and D. J. Singh, Phys. Rev. Lett. **72**, 3702 (1994).
[8] L. F. Mattheis, Phys. Rev. B **49**, 13 279 (1994).
[9] B. N. Harmon *et al.* (unpublished).
[10] S. A. Carter *et al.*, Phys. Rev. B **50**, 4216 (1994).
[11] J. S. Kim, W. W. Kim, and G. R. Stewart, Phys. Rev. B **50**, 3485 (1994).
[12] *Ternary Superconductors*, edited by G. K. Shenoy, B. D. Dunlap, and F. Y. Fradin (North-Holland, Amsterdam, 1981).
[13] *Topics in Current Physics*, edited by Ø. Fischer and M. B. Maple (Springer-Verlag, New York, 1983), Vols. 32 and 34.
[14] D. E. Moncton *et al.*, Phys. Rev. Lett. **45**, 2060 (1980).
[15] S. K. Sinha *et al.*, Phys. Rev. Lett. **48**, 950 (1982).
[16] See, for example, *High Temperature Superconductivity*, edited by J. W. Lynn (Springer-Verlag, New York, 1990), Chap. 8.
[17] T. E. Grigereit *et al.*, Phys. Rev. Lett. **72,** 2756 (1994).
[18] A. I. Goldman *et al.*, Phys. Rev. B **50**, 9668 (1994).
[19] G. E. Bacon, *Neutron Diffraction*, 3rd ed. (Clarendon, Oxford, 1975), Chap. 8.
[20] J. W. Lynn *et al.*, Phys. Rev. Lett. **46**, 368 (1981); J. W. Lynn *et al.*, *ibid.* **52**, 133 (1984).
[21] E. I. Blount and C. M. Varma, Phys. Rev. Lett. **42**, 1079 (1979).
[22] M. Tachiki, in *Ternary Superconductors*, edited by G. K. Shenoy, B. D. Dunlap, and F. Y. Fradin (North-Holland, Amsterdam, 1981), p. 267.